Rangin, C., Silver, E., von Breymann, M. T., et al., 1990
Proceedings of the Ocean Drilling Program, Initial Reports, Vol. 124

5. SUMMARY OF GEOPHYSICAL DATA FROM THE SULU AND CELEBES SEAS[1]

K. Hinz[2] and M. Block[2]

INTRODUCTION

A diversity of geophysical data exist from the Sulu and Celebes seas. Two seismic refraction profiles and magnetic surveyss were made by the *Vema* in 1967 (Murauchi et al., 1973). In 1974 the Comité d'Etudes Petroliers Marines conducted a multichannel seismic survey across the Sulu Sea (Mascle and Biscarrat, 1978). The Federal Institute for Geosciences and Natural Resources (BGR) collected 10,315 km of multichannel seismic data in parallel with magnetic and gravimetric measurements in the Sulu Sea and 580 km in the Celebes Sea on six cruises during the period from 1977 to 1987 (Table 1; Hinz et al., 1986; Dürbaum and Hinz, 1983). The oil industry surveyed approximately 18,000 km of multichannel seismic (MCS) data on the western Sulu shelf from 1965 to 1974 (Bell and Jessop, 1974).

Aeromagnetic measurements were carried out over the northwest Sulu Sea shelf (Bosum et al., 1972), and the U.S. Naval Oceanographic Office conducted a Project Magnet aeromagnetic survey of the central region of the Sulu Sea in 1987.

Heat-flow measurements (Tables 2 and 3) and sonobuoy seismic refraction measurements (Tables 4 and 5) were made in the Sulu Sea.

STRUCTURAL UNITS OF THE SOUTHEASTERN SULU BASIN

The main structural features observed in the Sulu Sea are shown in Figure 1. We identified five structural zones within the southeastern Sulu Basin on the basis of seismic interpretations. Some of these lines are shown in Figure 2 (back pocket).

Zone SES-I

Zone SES-I comprises the major portion of the deep southeastern Sulu basin. It lies between deep bathymetric depressions off the Sulu Archipelago and off Mindanao and Negros islands, and the steep southeast-facing flank of the Cagayan Ridge. A distinct N25°E-trending shear zone forms its western boundary. Zone SES-I is 130–140 km wide, but narrows east of 121.5°E toward the northeast. Its igneous basement is relatively smooth, and it has seismic characteristics typical of oceanic crust overlain by a 1–2-s (twt) thick sedimentary unit.

The dominant structural feature of Zone SES-I is a N 60°E-trending chain of basement highs. The largest observed basement high is 60 km long, 15 km wide, and approximately 1500 m high (Fig. 1). Basaltic rocks have been dredged from its eastern flank (Kudrass et al., this volume). The basement deepens from the chain of basement highs toward the southeast (i.e., toward the Sulu Archipelago and the islands of Mindanao, respectively; Fig. 1).

The heat-flow values are relatively high (Table 2). A distinct heat-flow anomaly with values ranging from 110 to 198 mW/m^2 coincides roughly with the eastern and southeastern boundary of Zone SES-I. Neither our own shipborne magnetic data nor the Project Magnet aeromagnetic data confirm the existence of northeast-trending magnetic lineations within Zone SES-I, described and interpreted by Lee and McCabe (1986) as magnetic lineations 17–20 (41–47 m.y.). Earthquakes are rare within Zone SES-I.

Zone SES-II

Zone SES-II is 7–25 km wide and comprises the more than 4550-m-deep bathymetric depressions off Mindanao and Negros islands that are trenches of an active subduction zone. The eastward- to southeastward-descending oceanic basement with dips of 11° is overlain by a 0.5–1.8-s (twt) sedimentary section. Temperatures of +10°C have been measured at the seabed, and heat-flow values ranging from 78 to 99 mW/m^2 have been determined within Zone SES-II. Sediments recovered by piston coring from this zone are finely laminated and multicolored, and are interpreted as turbidites (Kudrass et al., this volume). Zone SES-II terminates against Zone SES-III at about 9.5°N.

Zone SES-III

Zone SES-III is 15–35 km wide and is off the Sulu Archipelago east of 120°E, off Zamboanga Peninsula, and off Negros Island (Fig. 1). Its trend changes from N 60°E off the Sulu Archipelago to N-S at 7.5°N.

Zone SES-III is characterized by a series of imbricate thrust sheets forming a complex thrust system of predominantly sedimentary origin, as suggested from the derived normal moveout (NMO) velocities. The individual imbricate thrust sheets are separated by faults dipping to the southeast and east, respectively. The faults curve downward to a sole fault or major detachment plane that lies just above the descending igneous oceanic crust (Fig. 2 [back pocket] and Figs. 3 and 4).

The thickness of the complex thrust system comprising Zone SES-III increases landward to more than 4 s (twt), that is, about 6000 m. Zone SES-III can be described as an accretionary wedge resulting from active subduction of igneous oceanic crust, as indicated by the conspicuous bench-seafloor topography at the toe of the wedge and active seismicity.

Zone SES-III collides with the structural zone CA-I of the Cagayan terrane at 9.5°N, resulting in the formation of a distinct and complex anticlinal stack structure north of 9.5°N that continues northward into the Antique Range of western Panay Island. The latter is composed of a polymict melange that contains blocks of glaucophane schist, gabbro, peridotite, metavolcanics, and red chert embedded in a serpentinite matrix (McCabe et al., 1982). The Oligocene Panpanan Basalt occupies much of the northeast-trending Antique Range watershed west of the Iloilo Basin, according to Mitchell et al. (1986). North of 10°N, Zone SES-III is juxtaposed against and even thrust onto the Cagayan Ridge (Fig. 1).

The seismic data suggest that at least the southern offshore part of the Antique Ridge represents a collisional belt consisting of the accretionary wedge of structural Zone SES-III and the in-

[1] Rangin, C., Silver, E., von Breymann, M. T., et al., 1990. *Proc. ODP, Init. Repts.*, 124: College Station, TX (Ocean Drilling Program).
[2] Bundesanstalt für Geowissenschaften und Rohstoffe, D3000 Hannover 51, Postfach 510153, Federal Republic of Germany.

Table 1. Multichannel seismic, magnetic, and gravimetric surveys in the Celebes and Sulu seas.

Year	Vessel/ country	Cruise	Seismic source: Volume (in.^{3})	Seismic source: No. of guns	Receiver: Streamer length (m)	Receiver: No. of channels	Coverage (%)	Sonobuoy station no.	Gravity and magnetics	Total survey (km)
1974	*Lady Glorítta* France	CEPM	Vaporchoc		2,400	24	2,400			~ 600
1977	*Valdivia* F.R. Germany	VA-16	900	3	2,400	24	2,400	7	G, M	1,955
1982	*Sonne* F.R. Germany	SO-23	1,562	10	2,400 1,200	24 12	2,400 1,200	14	G, M	3,300
1983	*Sonne* F.R. Germany	SO-27	1,562	10	2,400	24	2,400		G, M	227
1984	*Explora* F.R. Germany	BGR-84	3,512	31	3,000	60	3,000			1,041
1986	*Explora* F.R. Germany	BGR-86	2,756	28	3,000	60	3,000		G, M	1,672
1987	*Sonne* F.R. Germany	SO-49	1,562	10	2,400	48	2,400		G, M	2,120
Celebes Sea										
1987	*Sonne* Germany	SO-49	1,562	10	2,400	48	2,400		G, M	580
									Σ	11,495

ferred volcanic Zone CA-I. North of 10°N, this complex collisional belt is juxtaposed and even thrust onto the Cagayan Ridge (Fig. 1).

Zone SES-IV

Zone SES-IV comprises an area of a particularly pronounced structural style. The 15–30-km wide zone extends over 300 km from the continental margin of southern Panay in the north, toward 7°30′S in the south (Fig. 1). Because of the lack of MCS data, it is uncertain whether this zone exists beneath the northern frontal portion of the Sulu Archipelago.

Zone SES-IV is characterized by three superimposed tectonic-stratigraphic units overlying actively subducting oceanic basement. The dominant tectonic-stratigraphic unit is a regional splinter characterized by high-amplitude reflections at the top and the base, and interval velocities of >4.5 km/s. The thickness of this regional splinter increases from less than 0.5 s (twt) at the front to 2.2 s (twt) toward the central Philippine Islands. Our seismic data strongly suggest that the splinter forms the "backstop" against which the previously discussed Zone SES-III accretes by the development of imbricate thrust sheets and simultaneous duplex-type shortening within the zone. By this process, mass is added to Zone SES-III resulting in thickening and progressive seaward growth of the zone as well as simultaneous uplift of the splinter.

The inferred oceanic crust slab is overlain by a sedimentary apron up to 2.4 s (twt) thick. The individual sedimentary sequence boundaries of this apron have a gentle dip of about 8° toward the east and downlap onto the top of the splinter (Fig. 2). Above the inferred hinge zone between the oceanic crustal splinter and the Philippine island arc (i.e. Zone SES-V) the apron sediments are folded and thrusted, resulting in the build-up of a complex anticlinal structure (Figs. 3 and 4). North of 9.5°N the sedimentary apron and also the underlying inferred oceanic crustal slab are affected by collision-related backthrusting. Apparently the sedimentary apron continues northward into the Iloilo basin of central Panay, which contains limestones, coarse clastic sediments, and interbedded basalt flows of Oligocene–lower Miocene age, overlain by a middle Miocene to Pliocene sequence of fine-grained sandstone and shale (McCabe et al., 1982).

Heat-flow values ranging from 45 to 70 mW/m^2 have been determined within Zone SES-IV, and the depths of the seismic epicenters are less than 75 km.

Zone SES-V

Zone SES-V comprises the western slope and shelf of Negros Island and of the Zamboanga Peninsula. A sedimentary apron with variable thickness ranging from a few hundred meters to 2.8 s (twt) overlies an acoustic basement complex, the surface of which is often characterized by a high-amplitude, discontinuous reflection horizon (Figs. 3 and 4).

The distinct acoustic basement complex of Zone SES-V presumably represents subsided parts of the Cretaceous melange basement, including overlying Oligocene to Miocene volcanic rocks of the Zamboanga Peninsula and of Negros Island. The melange basement of Zamboanga Peninsula includes chlorite and hornblende schists, metasandstone, phyllite, slate, marble, Cretaceous limestone, volcanic rocks, and lenses of serpentinized peridotite (Hamilton, 1979). Cretaceous sandstone, shale, spilite, and pillow basalt crop out in the southwest part of Negros Island, which otherwise consists mostly of Neogene andesitic volcanic rocks and their intrusive equivalents and derivative volcaniclastic sedimentary rocks (Hamilton, 1979).

REFERENCES

Bell, R. M., and Jessop, R.G.C., 1974. Exploration and geology of the west Sulu Basin, Philippines. *APEA J.*, 14:21–28.

Block, M., and Steinmann, D., 1988a. Geothermal studies. *In* Kudrass, H. R., et al. (Eds.), *Geological, Geochemical and Geothermal Investigations in the Sulu Sea/Phillipines (SO 49).* BGR Rep. 102042, Pt. 3 (Hannover, F. R. Germany).

Block, M., and Steinmann, D., 1988b. Geothermal studies. *In* Kudrass, H. R., et al. (Eds.), *Geological, Geochemical and Geothermal Investigations in the Sulu Sea/Phillipines (SO 58).* BGR Rep. 104774, Pt. 2 (Hannover, F. R. Germany).

Bosum, W., Fernandez, E., Kind, E., and Theodoro, C., 1972. Aeromagnetic survey of the Palawan Sulu offshore of the Philippines. *CCOP Tech. Bull.*, 6:141–160.

Dürbaum, H. J., and Hinz, K., 1983. SEATAR-related geophysical studies of the BGR in the Southwest Pacific. *Transactions, Circum-Pacific Energy and Mineral Resources Conference, 3rd, August 1982,* Honolulu, HI, 129–133.

Hamilton, W., 1979. Tectonics of the Indonesian region. *U.S. Geol. Surv. Prof. Pap.*, 1078.

Hinz, K., Kempter, E.H.K., Schlüter, H. U., 1986. The southern Palawan Balabac area: an accreted or non-accreted terrane? *Proc. Asian Council on Petroleum (ASCOPE) Conference and Exhibition, 3rd*, Dec. 1985, Kuala Lumpur, Malaysia, 2:48–72.

Hinz, K., and Schlüter, H. U., 1985. Geology of Dangerous Grounds, South China Sea, and the continental margin off Southwest Palawan—results of *Sonne* cruises, SO23 and SO27. *Energy*, 10:297–315.

Lee, C. S., and McCabe, R., 1986. The Banda-Celebes Sulu Basin: a trapped piece of Cretaceous-Eocene oceanic crust. *Nature*, 322:51–54.

Ludwig, W. J., Kumar, N., and Houtz, R. E., 1979. Profiler-sonobuoy measurements in the South China Sea basin. *J. Geophys. Res.*, 84: 3505–3518.

McCabe, P. R., Almasco, J., and Diegor, W., 1982. Geologic and paleomagnetic evidence for a possible Miocene collision in western Panay, central Philippines. *Geology*, 10:325–329.

Mascle, A., and Biscarrat, P. A., 1978. The Sulu Sea: a marginal basin in Southeast Asia. *In* Watkins, J. S., Montadert, L., and Dickerson, P. W., (Eds.), *Geological and Geophysical Investigation of Continental Margins.* AAPG Mem., 29:373–381.

Mitchell, A.H.G., Hernandez, F., and De la Cruz, A. P., 1986. Cenozoic evolution of the Philippine Archipelago. *J. Southeast Asian Earth Sci.*, 1:3–22.

Murauchi, S., Ludwig, W. J., Den, N., Hotta, H., Asanuma, T., Yoshii, T., Kubotera, A., and Hagiwara, K., 1973. Structure of the Sulu Sea and Celebes Sea. *J. Geophys. Res.*, 78:3437–3447.

Nagasaka, K., Francheteau, J., and Kishii, T., 1970. Terrestrial heat flow in the Celebes and Sulu seas. *Mar. Geophys. Res.*, 1:99–103.

Sclater, J. G., Karig, D., Lawver, L. A., and Louden, K., 1976. Heat flow, depth, and crustal thickness of the marginal basins of the South Philippine Sea. *J. Geophys. Res.*, 81:309–318.

Ms 124A-105

Table 2. Geothermal measurements in the southeast Sulu Sea Basin.

Number source	Name of station	Location N	Location E	Water depth (m)	Gradient (°C/cm × 10^3)	Conductivity (cal/cm · s · °C × 10^3) in situ	Conductivity core	Heat Flow (μcal/cm^2 · s)	Heat Flow (mW/m^2)
1/A	Circle 15	7°40.0′	121°28.0′	4974	1.06	2.1 (assumed)		2.2	92
2/A	Circle 16	8°21.1′	120°56.4′	4295	1.07	2.1 (assumed)		2.3	96
3/A	Circle 17	7°43.4′	119°34.8′	3675	1.23	2.1 (assumed)		2.6	108
4/B	A 181	7°17.6′	119°45.9′	3801	1.08	1.74 (assumed)		1.90	79
5/B	A 182	6°41.0′	120°09.0′	3641	1.02	—	1.74	1.77	74
6/B	T 01	8°17.5′	120°50.2′	3932	1.03	1.90 (assumed)		1.96	82
7/B	T 02	8°25.8′	121°43.1′	4857	0.31	1.90 (assumed)		0.59	25
8/C	HF 67/1	9°26.622′	121°54.619′	4023	0.48	2.23	2.05	1.07	45
9/C	HF 67/2	9°26.493′	121°54.628′	4017	0.49	2.13	2.05	1.04	43
10/C	HF 69	9°21.406′	121°38.678′	4635	1.09	2.17	2.10	2.37	99
11/C	HF 76/1	9°16.687′	121°32.067′	4642	1.91	2.30	2.18	4.39	183
12/C	HF 76/2	9°16.611′	121°32.103′	4650	2.09	2.27	2.18	4.74	198
13/C	HF 81/1	8°09.808′	121°36.383′	4804	1.60	2.15	2.14	3.44	143
14/C	HF 81/2	8°09.902′	121°36.336′	4835	1.48	2.17	2.14	3.21	134
15/C	HF 92	8°01.43′	121°56.96′	3986	0.56	2.84	2.43	1.59	66
16/C	HF 97	8°11.00′	119°28.32′	3564	1.07	1.97	1.91	2.11	88
17/D	41HF-1	9°56.09′	121°39.09′	3758	0.40	2.21	—	0.88	37
18/D	41HF-2	9°56.51′	121°39.57′	3755	0.34	2.15	—	0.73	30
19/D	50HF-1	9°16.35′	121°29.84′	4379	1.66	2.18 (assumed)		3.62	151
20/D	50HF-2	9°16.46′	121°30.12′	4398	1.79	2.18	—	3.90	163
21/D	50HF-3	9°16.34′	121°30.41′	4420	2.11	2.18 (assumed)		4.60	192
22/D	50HF-4	9°16.37′	121°30.87′	4494	1.39	2.27	—	3.16	131
23/D	55HF-1	9°23.42′	121°40.14′	4567	0.98	2.22	—	2.18	91
24/D	55HF-2	9°22.02′	121°39.83′	4611	0.99	2.51	—	2.48	104
25/D	55HF-3	9°22.64′	121°39.54′	4611	0.92	2.40	—	2.21	92
26/D	55HF-4	9°22.66′	121°39.00′	4585	1.09	2.19	—	2.39	99
27/D	55HF-5	9°22.37′	121°38.47′	4570	1.04	2.17	—	2.26	94
28/D	55HF-6	9°22.09′	121°37.97′	4659	1.16	2.11	—	2.45	102
29/D	55HF-7	9°21.70′	121°37.43′	4696	1.11	2.15 (assumed)		2.39	99
30/D	60HF	9°14.10′	121°25.40′	4063	0.38	2.14	—	0.81	34
31/D	61HF	9°09.2′	121°17.1′	3693	0.76	2.04	—	1.55	65
32/D	62HF	9°05.26′	121°11.44′	3920	1.03	2.15 (assumed)		2.21	92
33/D	68HF	8°49.80′	121°20.00′	3350	0.40	2.01	—	0.80	34
34/D	70HF	8°49.80′	121°35.40′	4726	1.71	2.18	—	3.73	155
35/D	75HF	9°21.19′	121°35.74′	4700	1.09	2.15 (assumed)		2.34	98
36/D	79HF-1	8°24.50′	121°10.46′	4270	1.09	2.05	—	2.23	93
37/D	79HF-2	8°24.70′	121°10.70′	4270	1.08	2.03	—	2.19	91
38/D	81HF	7°59.70′	121°15.00′	4320	1.29	2.05	—	2.64	110
39/D	84HF	8°08.60′	121°39.00′	4870	0.90	2.09	—	1.87	78
40/D	85HF	8°09.03′	121°41.49′	4870	0.98	2.08	—	2.04	85
41/D	87HF	8°02.50′	121°53.90′	3906	0.58	2.26	—	1.31	55
42/D	91HF	8°15.60′	121°30.57′	4460	1.11	2.12	—	2.35	98
43/D	92HF	8°12.75′	121°34.15′	4560	1.28	2.11	—	2.70	113
44/D	99HF	8°09.00′	121°44.50′	4680	0.97	2.00	—	1.94	81
45/D	100HF	8°08.77′	121°47.40′	4498	0.78	1.95	—	1.52	63
46/D	103HF	8°09.24′	121°38.70′	4870	1.38	2.11	—	2.91	121

Sources: A = Nagasaka et al., 1970; B = Sclater et al., 1976; C = *Sonne* cruise SO-49, Block and Steinmann, 1988a; and D = *Sonne* cruise SO-58, Block and Steinmann, 1988b.

Table 3. Geothermal measurements in the northwest Sulu Sea Basin.

Number source	Name of station	Location N	Location E	Water depth (m)	Gradient (°C/cm × 10^3)	Conductivity (cal/cm · s · °C × 10^3) in situ	Conductivity core	Heat Flow (μcal/cm^2 · s)	Heat Flow (mW/m^2)
47/C	HF 46/1	10°01.395′	120°29.474′	1542	0.71	1.94	2.14	1.38	58
48/C	HF 46/2	10°01.352′	120°29.637′	1542	0.74	2.10	2.14	1.55	65
49/C	HF 51/1	10°21.308′	121°20.763′	1167	0.82	2.06	1.95	1.69	70
50/C	HF 51/2	10°21.077′	121°20.363′	1170	0.80	2.08	1.95	1.66	69
51/C	HF 114	8°04.411′	118°19.156′	461	0.50	2.32	2.06	1.16	48

Source: C = *Sonne* cruise SO-49, Block and Steinmann, 1988a.

Table 4. Refraction seismic and sonobuoy measurements in the northwest Sulu Sea.

Name of station	Source	Location N	Location E	Water depth (m)	V_1 h_1	V_2 h_2	V_3 h_3	V_4 h_4	V_5 h_5	V_6 h_6	V_7 h_7	V_8 h_8
					1.90*	3.10	4.82*	5.65	6.72			
Profile 15	A	09°29′	119°09′	2030	3.00	4.58	1.29	3.77				
		08°51′	119°15′	2030	1.10	0.70	4.16	3.79				
					2.20	2.95	3.45	3.85				
307C12	B	07°15.2′	118°05.6′	90	1.18	1.03	1.35					
					2.10	2.55	3.20	4.20				
308C12	B	06°50.8′	118°15.3′	80	1.13	0.49	1.54					
					2.15	2.40	2.60	4.90				
43C14	B	07°57.0′	117°11.5′	190	0.51	1.01	1.26					
					1.92	2.24	3.89	4.25	4.76	5.86		
SB-I	C	10°14.49′	119°50.62′	110	0.10	0.48	0.18	0.94	1.49			
					1.74	1.97	2.72	2.95	3.94	4.5		
SB-II	C	10°20.98′	120°05.46′	190	0.05	0.28	0.73	1.38	0.34			
					2.30	2.77	3.47	4.03				
SB-III	C	10°00.29′	120°36.31′	1540	1.59	0.70	2.06					
					2.12	2.55	3.02	3.54	4.16	6.66		
SB-IV	C	09°44.02′	119°51.89′	1170	1.48	1.35	0.35	1.72	1.85			
					1.90	2.21	2.42	4.21	4.95			
SB-V	C	09°18.07′	118°49.92′	1970	1.12	0.04	2.18	1.29				
					1.94	2.32	3.06	3.66	4.44	4.86		
SB-VI	C	08°44.84′	119°16.09′	2000	0.76	0.15	0.85	1.59	0.94			
					2.00	2.32	2.68	3.16	3.58	3.74		
SB-VII	C	08°25.59	118°15.80′	810	0.49	0.93	0.82	0.51	1.13			
					1.96	2.38	3.00					
SB-VIII	C	08°22.40′	118°34.16′	1590	0.92	1.43						
					2.37	2.87	3.68	4.63	5.19			
SB-IX	C	08°55.23′	119°24.92′	1970	1.65	0.12	1.67	2.74				
					2.39	2.83	3.22	3.81	4.44			
SB-XII	C	09°03.82′	119°23.72′	1920	2.04	0.17	0.43	1.91				
					1.74	1.83	2.15	2.38				
SB-XIII	C	09°21.32′	119°15.96′	2000	0.91	0.09	0.59					
					1.60	2.10	2.90	3.25	4.55			
SB-20	D	08°59.49′	119°20.62′	2000	0.64	0.53	0.70	2.26				
					1.55	2.30	2.50	2.70				
SB-22	D	09°28.72′	119°58.98′	1340	0.57	0.59	0.75					
					1.58	1.80	2.30	2.80	3.80			
SB-23	D	09°47.02′	120°27.20′	1540	0.56	0.12	0.63	1.11				

Note: V = seismic velocity in km/s (V* = assumed velocity), and h = thickness in kilometers, of the isovelocity layers derived from the seismic measurements.

Sources: A = Murauchi et al., 1973; B = Ludwig et al., 1979; C = *Sonne* cruise SO-23, H. S. Schröder, unpubl. data; and D = *Valdivia* cruise VA-16, H. Schröder, unpubl. data.

Table 5. Refraction seismic and sonobuoy measurements in the southeast Sulu Sea.

Name of station	Source	Location N	Location E	Water depth (m)	V_1 h_1	V_2 h_2	V_3 h_3	V_4 h_4	V_5 h_5	V_6 h_6	V_7 h_7	V_8 h_8
					2.00*	3.4*	6.41	8.28				
Profile 16	A	07°48′	120°04′	3900	0.53	2.24	4.01					
		07°21′	120°30′	4270	1.10	2.04	3.86					
					2.00*	3.51	5.18	6.16	7.19			
Profile 17	A	06°43′	121°17′	50	0.05	1.34	2.92	5.02				
		06°18′	121°38′	50	0.11	1.81	1.85	5.02				
					2.05	2.45	2.75	3.10	3.50	3.80		
309C12	B	06°27.9′	118°52.8′	620	1.10	0.41	0.61	0.39	0.65			
					1.90	2.05	2.85					
310C12	B	05°59.8′	119°20.2′	980	0.79	1.12						
					1.67*	2.35*	4.45					
41C14	B	05°38.5	119°48.8	470	0.73	1.73						
					1.8*	2.65						
42C14	B	05°49.8*	119°53.6′	540	1.10							
					1.74*	2.28*	3.14*	4.60				
215V28	B	07°54.2′	120°06.7′	4040	0.43	0.48	0.89					
					1.75	2.05	2.20	2.55	2.75	4.90	7.50	
SB X	C	06°12.33′	119°08.47′	670	0.50	0.21	0.77	1.01	3.67	3.25		
					1.83	3.00	3.94	4.67	5.50			
SB XI	C	06°21.57′	119°25.87′	2950	0.92	1.34	0.82	0.64				

Note: V = seismic velocity in km/s (V* = assumed velocity), and h = thickness in kilometers of the isovelocity layers derived from the seismic measurements.
Sources: A = Murauchi et al., 1973; B = Ludwig et al., 1979; and C = *Sonne* cruise SO-23, H. Schröder, unpubl. data.

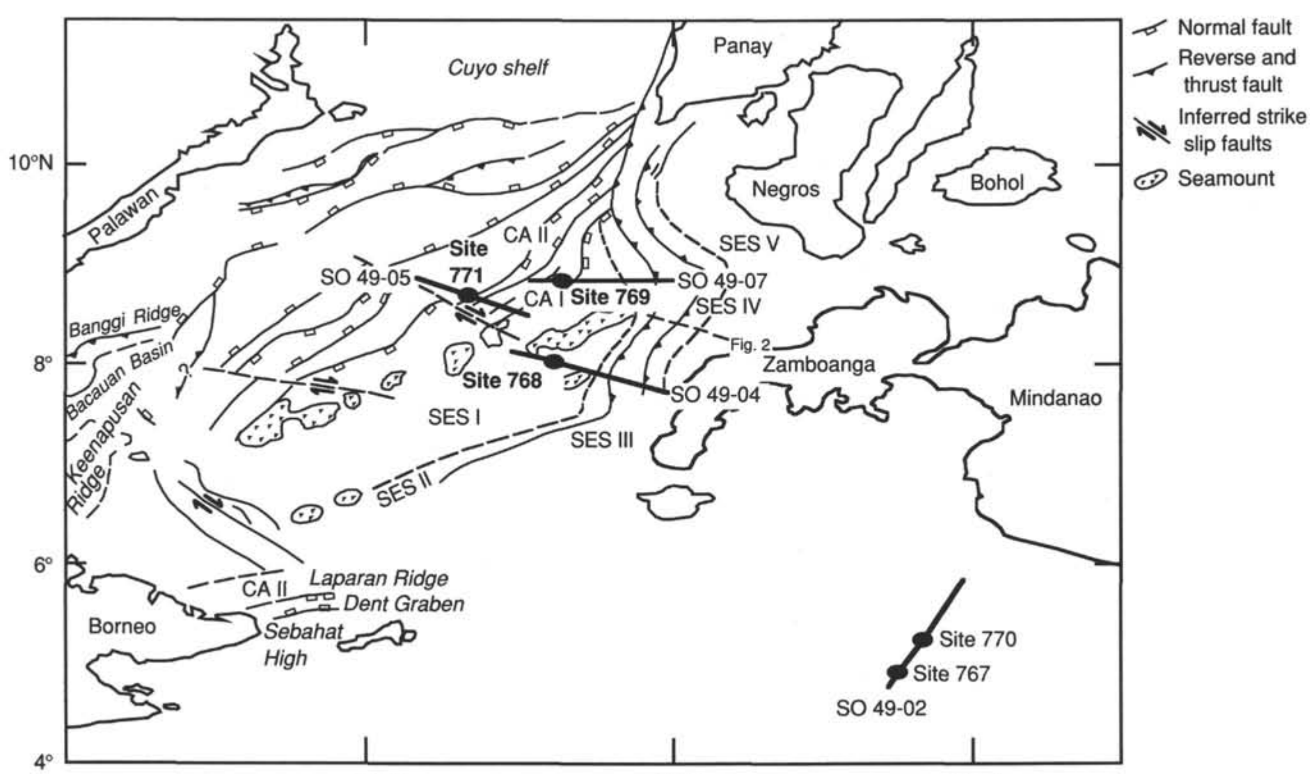

Figure 1. Structural map of the southeast Sulu Sea based on seismic line interpretation.

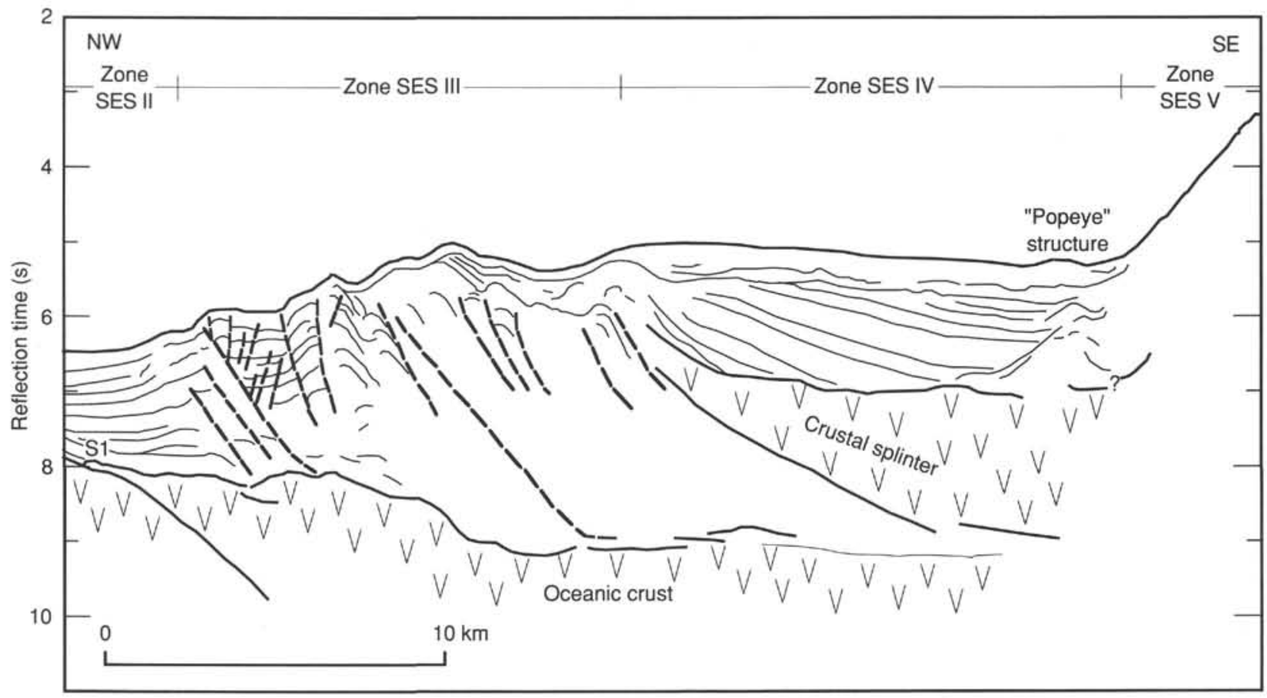

Figure 3. Interpretation of Line SO49-06 (SP-255-1000) showing presence of a crustal splinter in the Sulu Sea Trench inner wall (location on Fig. 1).

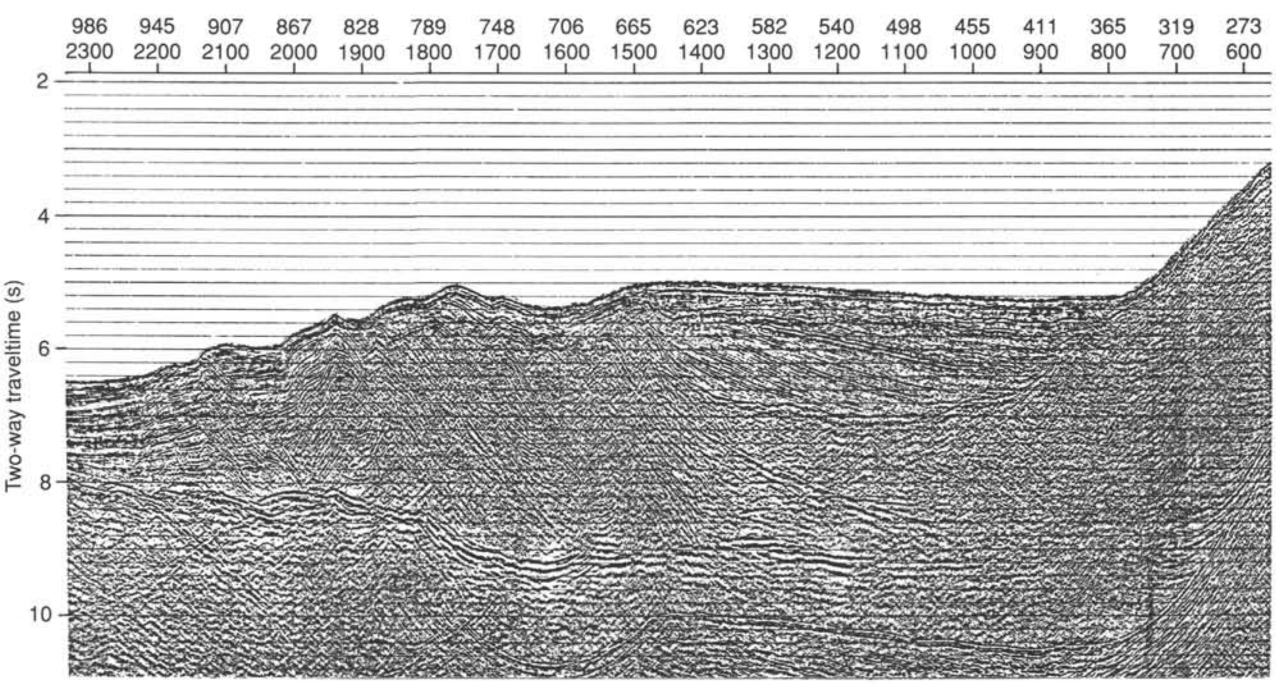

Figure 4. Seismic record of Line SO49-06 (SP-255-1000). Location on Figure 1.